AJNR

MR Imaging of the Trigeminal Ganglion, Nerve, and the Perineural Vascular Plexus: Normal Appearance and Variants with Correlation to Cadaver Specimens

Lorna Sohn Williams, Ilona M. Schmalfuss, Christopher L. Sistrom, Takuya Inoue, Ryusui Tanaka, Eduardo R. Seoane and Anthony A. Mancuso

AJNR Am J Neuroradiol 2003, 24 (7) 1317-1323
http://www.ajnr.org/content/24/7/1317

AJNR Am J Neuroradiol 24:1317–1323, August 2003

MR Imaging of the Trigeminal Ganglion, Nerve, and the Perineural Vascular Plexus: Normal Appearance and Variants with Correlation to Cadaver Specimens

Lorna Sohn Williams, Ilona M. Schmalfuss, Christopher L. Sistrom, Takuya Inoue, Ryusui Tanaka, Eduardo R. Seoane, and Anthony A. Mancuso

BACKGROUND AND PURPOSE: **MR imaging is the method of choice for evaluating the trigeminal nerve. Detection of abnormalities such as perineural tumor spread requires detailed knowledge of the normal MR appearance of the trigeminal nerve and surrounding structures. The purpose of this study was to clarify the normal MR appearance and variations of the trigeminal ganglion, maxillary nerve (V2), and mandibular nerve (V3) with their corresponding perineural vascular plexus.**

METHODS: **MR images obtained in 32 patients without symptoms referable to the trigeminal nerve were retrospectively reviewed. The trigeminal ganglion in Meckel's cave, V2 within the foramen rotundum, and V3 at the level of foramen ovale were assessed for visualization and enhancement. The configuration of the perineural vascular plexus was recorded. Correlation to cadaver specimens was made.**

RESULTS: **The trigeminal ganglion and V3 were observed to enhance in 3–4% of patients unilaterally. V2 and V3 were well visualized 93% of the time. The perineural vascular plexus of V2 was observed 91% of the time, and that of V3 in 97% of instances.**

CONCLUSION: **This study characterizes the normal MR appearance of the trigeminal ganglion and its proximal branches. The trigeminal ganglion, V2, and, V3 are almost always reliably seen on thin-section MR studies of the skull base. Enhancement of the perivascular plexus is routinely seen; however, enhancement of the trigeminal ganglion, V2, or V3 alone is seen only on occasion as supported by the avascular appearance of these anatomic structures in cadaver specimens.**

The trigeminal nerve is the largest cranial nerve (1). It is commonly involved in a variety of disease processes that may be visualized with modern imaging techniques (2–4). MR imaging is considered the primary method for evaluating patients with symptoms related to the trigeminal nerve in most clinical settings (5). Previous literature demonstrated the ability of cross-sectional imaging to depict the anatomy of the trigeminal ganglion (or semilunar or gasserian ganglion) in Meckel's cave (6–9). Although the normal anatomic appearance of the trigeminal ganglion and the proximal divisions of the trigeminal nerve have been illustrated in the literature, to our knowledge a detailed MR imaging description with cadaver correlation of the perineural vascular plexus surrounding the trigeminal ganglion and the divisions of the trigeminal nerve as they exit the skull base has not been described. A clear understanding of the anatomic relationship and variations between the trigeminal ganglion-nerve complex and its perineural vascular plexus is critical for accurate assessment and detection of disease related to the trigeminal nerve. Furthermore, a lack of knowledge of the normal enhancing pattern of the perineural vascular plexus may result in mistaking this normal enhancement for enhancement of the ganglion itself, as suggested in a previous study (10).

The purpose of this study was to establish and clarify the normal MR imaging appearance and vari-

Received July 17, 2002; accepted with revisions February 12, 2003.

From the Department of Radiology (L.S.W.), JFK Medical Center, Atlantis, FL; and the Departments of Radiology (I.M.S., C.L.S., A.A.M.) and Neurosurgery (T.I., E.R.S.), University of Florida College of Medicine, Gainesville, FL

Address correspondence to Anthony A. Mancuso, M.D., Professor and Chairman, Department of Radiology, University of Florida College of Medicine, P.O. Box 100374, 1600 SW Archer Road, Gainesville, FL 32610-0374.

ations of the trigeminal ganglion-nerve complex and its corresponding perineural vascular plexus and to support the imaging results with findings from cadaver specimens.

Methods

MR Assessment of the Trigeminal Ganglion and Proximal Maxillary Nerve and Mandibular Nerve

A list was compiled of all adult patients (age range, 18–82 years) referred from January 1997 to January 1998 for MR imaging because of suspected pituitary disease, sensorineural hearing loss, or vision loss. Any patient with a history of trigeminal nerve symptomatology, previous radiation treatment, brain surgery, CNS infection, inflammation, or neoplasm was excluded from the study. MR findings in 36 patients were retrospectively reviewed for image quality. Four patients were excluded from the final imaging analysis because of motion artifacts impeding evaluation of the trigeminal ganglion and its proximal divisions. The MR images of 32 patients (16 male patients, 16 female patients; age range, 18–82 years [mean, 55.3 years]) were reviewed and analyzed on a PACS workstation. The images were reviewed independently by an attending neuroradiologist (L.S.W.) and a neuroradiology fellow (I.M.S).

Conventional and fast spin-echo images were acquired in the axial and coronal planes with 3- or 4-mm contiguous sections and a 16- to 18-cm field of view. T1-weighted imaging was performed before and after gadolinium administration. Pre- and postgadolinium T1-weighted images were acquired with a TR of 400–630 ms and TE of 12 or 15 ms. Fat-suppression sequences were not used to evaluate the ganglion, maxillary nerve (V2), and mandibular nerve (V3), because of the unpredictable occurrence of susceptibility artifacts at the skull base and their containment of air-bone interfaces. All imaging examinations were performed on a Siemens 1.5-T Vision or Siemens 1.0-T Magnetom unit (Siemens Corporation, Erlangen, Germany) or a GE 1.5-T Signa (General Electric Medical Systems, Inc., Milwaukee, WI).

The trigeminal ganglion at its anterior inferior limit within the trigeminal cistern (Meckel's cave) was evaluated in the coronal plane. V2 was surveyed at its most anterior aspect within foramen rotundum in the coronal plane, and V3 was evaluated at the level of foramen ovale in the coronal plane. Both sides of the ganglion, V2, and V3 in all patients were independently evaluated by the two observers.

Enhancement within the ganglion, V2, and V3 was assessed qualitatively, with enhancement defined as signal intensity similar to that of the pituitary gland. The configuration of the perineural vascular plexus surrounding the ganglion, V2, and V3 was also assessed. Specifically, the trigeminal ganglion was scored qualitatively (yes or no) with regard to whether it was seen as a discrete structure and whether it enhanced. Qualitative assessment of V2 and V3 included visualization (yes or no), morphology (only the nerve was seen, nerve and vascular plexus were seen as separate structures, enhancing nerve was seen with no clear distinction of the vascular plexus), and relationship of plexus to the nerve (plexus completely or incompletely surrounding the nerve, as in the case of V2; plexus seen only on one or both sides of nerve for V3). The nerve-plexus complexes in total and the nerves (V2 and V3) alone were measured on gadolinium-enhanced coronal T1-weighted images with electronic calipers along their greatest diameters within the central aspect of the foramen rotundum and ovale, respectively.

Evaluation of Trigeminal Ganglion and Proximal V2 and V3 in Cadavers

One or both sides of 10 adult cadaver specimens were examined, which yielded 12 specimens (both sides of two cadavers were used). The formalin-fixed cadaver heads were injected with colored silicon solution to distinguish between arteries and veins (11). The carotid and vertebral arteries were injected with red- and the jugular veins with blue-colored solution (11). Microdissection was performed by using a Zeiss operating microscope, model OPMI-FC (11). The trigeminal nerve was divided into three components in the paracavernous sinus regions: the trigeminal ganglion within the inferior aspect of the trigeminal cistern and the proximal portion of V2 and V3 (11). The extent (complete or incomplete) of the perineural vascular plexus surrounding the ganglion and the proximal nerve branches was assessed visually.

Statistical Analysis

Statistical calculations were done with SAS version 8 (SAS Institute, Cary, NC). All tests for statistical significance were performed for two-tailed hypotheses with á = 0.05. Descriptive statistics for the qualitative data were developed after pooling right and left sides as scored by both observers. Similarly, the quantitative measurements of nerve-plexus sizes were averaged across sides and observers. This was done to simplify the presentation of results. Confidence intervals (95%) were calculated as appropriate to the variable in question.

Interobserver agreement on qualitative assessments of the ganglia, V2, and V3 was tested by using the κ statistic (weighted when appropriate) paired across observers. Interobserver agreement for the measurements of V2 and V3 (nerve and nerve-plexus complex) was determined with intraclass correlation coefficient. These were calculated from the mean squares between subjects and for error obtained with analysis of variance on each of the four measurements.

Side to side symmetry of the qualitative assessments was evaluated on paired (left and right) data by using McNemar's test (12). Percent concordant (number of subjects in whom left and right agree divided by total) was also calculated. For the quantitative measurements of V2 and V3 nerve or nerve-plexus diameters, paired t testing was used to assess both interobserver and side to side differences. Because the alternate hypothesis was set to be differences between paired observations, low P values would indicate poor reliability or asymmetry, respectively.

The addition of proportional agreement rather than κ for symmetry of observational findings was made, because calculating and interpreting the κ statistic tends to be problematic when one or more cells in the contingency table are null (ie, sparse tables [13]). Similar problems may arise when the observations are crowded into one diagonal corner of the table. One or both of these situations occurred in more than half of the calculations.

Results

MR Imaging of the Trigeminal Ganglion, V2, and V3

The results for visualization of the ganglion and nerve, enhancement pattern, and the nerve and nerve-plexus diameters are summarized in Table 1. The interobserver reliability for visualizing the structures, assessing morphology, and determining enhancement of the ganglion, V2, and V3 is listed in Table 2. The κ scores ranged from 0.41 for visualization of V3 to 0.79 for assessing morphology of the ganglion. The κ scores for interobserver reliability concerning qualitative observations of ganglion and nerve branches (Table 2) may seem somewhat low. This, however, is largely due to the way in which the κ statistic is calculated, combined with structure of

TABLE 1: Qualitative findings and measurements

Finding	Ganglion	V2	V3
Visualized	98% (95–100)	93% (88–100) (Fig 9)	93% (88–100)
Only nerve seen	NA	9% (2–17)	3% (0–7)
Nerve and plexus seen as distinct structures	NA	91% (83–98)	97% (93–100)
Enhancing ganglion or nerve seen with no distinct vascular plexus	4% (0–10)	18% (9–28)	3% (0–7)
Plexus completely surrounding V2 or seen on both sides of V3	NA	41% (29–53)	75% (64–87)
Combined diameter of nerve and plexus when seen as distinct structures (mm)	NA	3.0 ± 0.53 (2.9–3.1)	3.9 ± 0.84 (3.7–4.1)
Diameter of the nerve alone (mm)	NA	1.6 ± 0.48 (1.5–1.7)	1.9 ± 0.67 (1.8–2.0)

Note.—Qualitative results are reported as percentages. Sizes are reported as mean ±SD. CI (95% lower-upper) are provided for all results in parenthese.

TABLE 2: Interobserver reliability of qualitative findings and measurements

Finding	Ganglion	V2	V3
Visualization*	0.66 (98%)	0.64 (95%)	0.41 (92%)
Morphology and enhancement*	0.79 (98%)	0.56 (81%)	0.55 (95%)
Plexus completely surrounding V2 or seen on both sides of V3*	NA	0.74 (86%)	0.65 (87%)
Diameter of nerve and plexus (mm)†	NA	0.83	0.79
Diameter of nerve alone (mm)†	NA	0.72	0.85

* κ statistic and percent agreement (in parentheses) for qualitative findings.
† Intraclass correlation coefficient for measured diameters.

TABLE 3: Left-right symmetry of qualitative findings and measurements

Finding	Ganglion	V2	V3
Visualized*	$P = 1.0$, agree = 0.92	$P = .51$, agree = 0.86	$P = .51$, agree = 0.86
Morphology and enhancement*	$P = .37$, agree = 0.92	$P = .16$, agree = 0.75	$P = .39$, agree = 0.91
Plexus completely surrounding V2 or seen on both sides of V3	NA	$P = 1.0$, agree = 0.49	$P = 1.0$, agree = 0.62
Diameter of nerve and plexus (mm)	NA	$P = .36$, diff = 0.07	$P = .23$, diff = 0.16
Diameter of nerve and alone (mm)	NA	$P = .12$, diff = 0.13	$P = .57$, diff = 0.05

Note.—Reported *P* values for significant different between left and right from McNemar's test for qualitative findings (indicated by asterisks) and paired t tests for measurements. Agree indicates proportion concordant (sides in agreement/total); diff, mean difference in millimeters (right-left).

our data. Specifically, this problem occurs when a 2 × 2 table of interobserver agreement is heavily weighted into one cell of main diagonal. For example, with respect to the ganglion, both observers reported that they saw the structure 62 times in 64 observations. This translated into a high expectation of agreement by chance alone (95.4%). Because the κ statistic quantifies the improvement on the basis of chance, going from 95.4% to 98% (the observed agreement) yields a statistic of only 0.66, despite that agreement is nearly perfect. In essence, observers are not "credited" by κ for agreeing with each other that the ganglion is visible most of the time.

Reliability of measuring diameters of the nerve and nerve-plexus complex is also listed in Table 2. The ganglia and nerves were bilaterally symmetric in terms of visualization, enhancement, and measured size (Table 3). This is evidenced by *P* values for paired right to left differences calculated by McNemar's method (0.16–1.0) and paired *t* tests (0.12–0.57) that were all well above .05. Had there been any significant asymmetry of observed findings or measurements, at least one of the tests would have yielded a significant ($P < .05$) result. For qualitative findings, the proportion of left-right concordance was moderate to high (>0.70) for all observations, except for completeness of the plexus of V2 (0.49) and V3 (0.62). Therefore, although configuration of the V2 and V3 plexus often differed from side to side, no tendency existed for one side to be complete more often than the contralateral side. The right-left differences of all four measured diameters of the neurovascular structures (around .2 mm) fell well within the range of measurement error.

Trigeminal Ganglion, V2, and V3 in Cadavers

In the cadaver heads, a constant and extensive pericavernous venous plexus was identified that surrounded the trigeminal ganglion in all specimens examined (Fig 1). These cavernous channels coursed along the lateral margin of the sella, the medial aspect of the middle fossa, the inferior orbital fissure, and the foramina ovale, rotundum, and spinosum (11). The venous plexus was seen outside the cavernous sinus located in a dural envelope that makes up the lateral wall of the cavernous sinus (11). It showed direct connections to the cavernous sinus. In two (16.6%) of 12 sides examined, a distinct vascular plexus was not demonstrated around V2 or V3. Complete dissection and removal of the perineural vascular plexus, when present, revealed the trigeminal ganglion and proximal divisions of the trigeminal nerve to

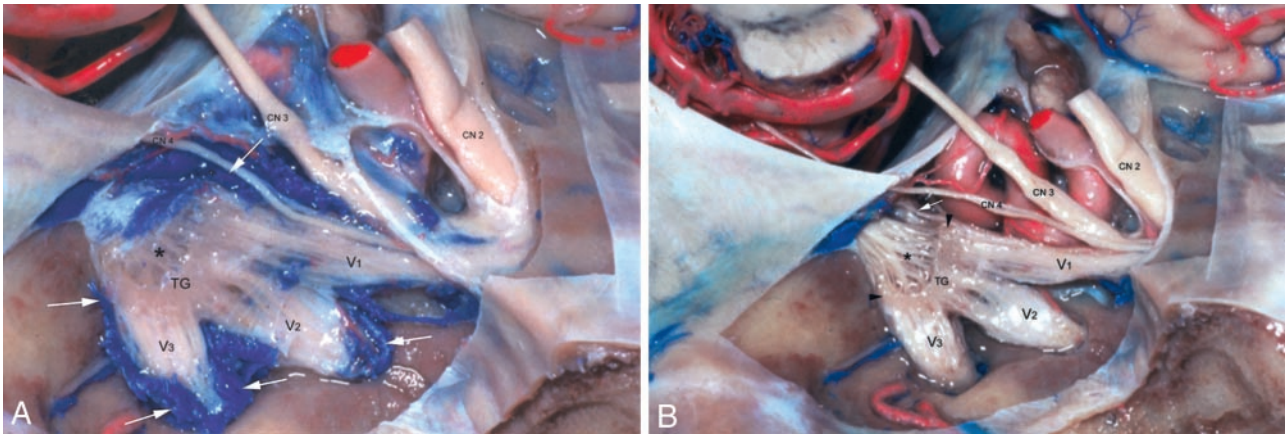

FIG 1. Trigeminal ganglion in trigeminal cistern in cadaver.

A, Trigeminal ganglion (TG) is crescentic in shape and proximal divisions of trigeminal nerve (V1, V2, V3) emerge from its anterolateral border. The trigeminal rootlets (*) enter the crescent-shaped TG. V1 exits the TG as the most superior branch. It lies immediately inferior to cranial nerve four (CN4). V2 leaves TG as the middle branch and V3 as the most inferior division. Venous structures are blue- and arterial red-colored silicon. An extensive pericavernous venous plexus surrounds the ganglion and each of the trigeminal nerve branches (*white arrows*).

B, Following dissection of the pericavernous venous plexus, the avascular nature of the trigeminal ganglion and its proximal divisions (V1, V2, V3) is seen. The extent of the trigeminal ganglion (between *arrowheads*) and the trigeminal nerve rootlets (*) are now better delineated. The cranial nerve six (*white arrow*) is now visible inferior medial to V1. CN indicates cranial nerve

be devoid of obvious vascularity in all specimens examined (Fig 1B).

Comparison of MR Imaging and Cadaver Specimen Results

Comparison of cadaver dissections to MR imaging findings of the trigeminal ganglion and proximal division of V2 and V3 revealed that the perineural vascular plexus present in cadaver specimens (Fig 1) corresponded well to the perineural vascular plexus surrounding the trigeminal ganglion and the proximal divisions of V2 and V3 as they exited through the foramen rotundum and ovale, respectively (Figs 2, 3, and 4). A distinct plexus surrounding V2 and V3 was absent in two of the 12 sides in the cadavers. This may be related to normal variation, because the vascular plexus was not seen surrounding V2 and V3 at MR imaging 9% and 3% of the time, respectively. In addition, the perineural venous plexus was seen as an incomplete structure surrounding V2 (Fig 5) and V3 in 59% and 75%, respectively. The cadaver specimens could not be evaluated for completeness of the plexus, because the plexus was fragile and therefore difficult to remove in on piece.

Discussion

Anatomy of the Trigeminal Ganglion-Nerve Complex and the Vascular Plexus

The trigeminal nerve has three main branches: V1, V2, and V3. V1 is purely sensory and the smallest division. It provides sensory innervation to the eye, orbit, and forehead. Just posterior to the orbital apex, the branches of V1 coalesce to form the V1 trunk. V1 travels in the lateral wall of the cavernous sinus posteriorly below the oculomotor and trochlear nerves (14, 15).

V2 is also purely sensory and provides sensory innervation from the maxilla, palate, upper lip, cheek, nasal cavity, nose, and nasopharynx. The branches of V2 merge within the infraorbital canal and in the pterygopalatine fossa to form V2. It travels through the foramen rotundum to enter the cavernous sinus (14, 15).

V3 is both motor and sensory and is the largest division. V3 supplies sensation to the chin, lower lip, floor of mouth, tongue, side of head and scalp, and meninges. Regarding the motor root, read further. The sensory branches of V3 coalesce within the parapharyngeal space just below the skull base to form V3. V3 ascends between the tensor veli palatini and the lateral pterygoid muscles and travels through the skull base within the foramen ovale (14, 15).

V1, V2, and V3 merge within the posterior aspect of the cavernous sinus to form the sensory trigeminal ganglion. The trigeminal ganglion is located in the anterior inferior aspect of a dural pouch called the trigeminal cistern situated in a small depression in the petrous apex known as Meckel's cave (7). The leptomeninges forming the trigeminal cistern have three finger-line projections that accompany V1, V2, and V3 nerves as they course through their respective foramina (3, 16). The ganglion then separates into multiple individual rootlets that course through the trigeminal cistern posteriorly. The trigeminal nerve fascicles enter the prepontine cistern through the porus trigeminus, an oval opening found beneath the free edge of the tentorium at the petrous apex (7, 16–18). The fascicles reach the root entry zone of the trigeminal nerve (the most posterior centimeter of the nerve before it enters the pons) at the ventrolateral surface of the pons.

The sensory fibers break away to reach the three different sensory brain stem nuclei of the trigeminal nerve. The central brain stem nuclei extend from the

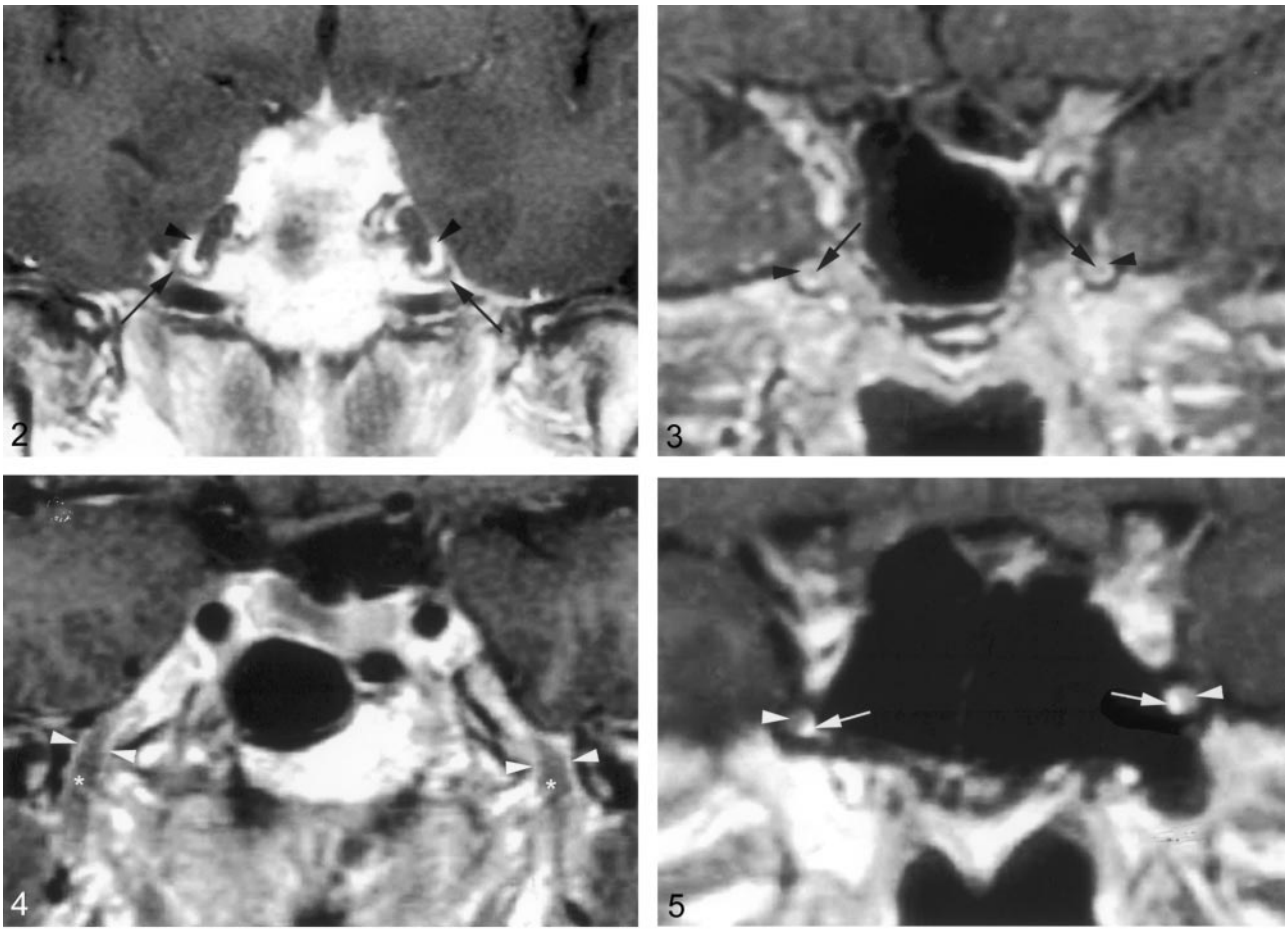

FIG 2. Coronal gadolinium-enhanced T1-weighted image (TR/TE/NEX, 400/15/2) depicts the nonenhancing crescent-shaped trigeminal ganglion (*arrows*) and the prominent perineural venous plexus (*arrowheads*) superior to it. The venous plexus as well as the ganglion are symmetric in appearance.

FIG 3. Coronal gadolinium-enhanced T1-weighted image (TR/TE/NEX, 500/15/2) illustrates the common appearance of V2 (*arrows*) within the foramen rotundum as central nonenhancing nerve completely surrounded by the perineural venous plexus (*arrowheads*).

FIG 4. Coronal gadolinium-enhanced T1-weighted image (TR/TE/NEX, 500/15/2) illustrates the normal appearance of V3 as it exits the skull base through the foramen ovale. V3 (*) is surrounded by the venous plexus (*arrowheads*) on both sides at the level of the foramen ovale and over a short distance below the skull base. The perineural venous plexus (*arrowheads*) demonstrates the same thickness on each side of the nerve.

FIG 5. Coronal gadolinium-enhanced T1-weighted image (TR/TE/NEX, 500/15/2) shows an incomplete perineural venous plexus within the foramen rotundum as an anatomic variant. Only small portion of the perineural venous plexus (*arrowheads*) is seen medial to V2 (*arrows*) on both sides.

midbrain to medulla (19): the mesencephalic nucleus lateral to the cerebral aqueduct, the principal sensory nucleus in the dorsolateral area of the pontine tegmentum at the level of the entry zone of the sensory fibers, and the spinal nucleus in the inferior part of the pons and throughout the medulla (19). In addition, there is a motor nucleus in the superior part of the pons, deep to the floor of the fourth ventricle (19). It gives rise to the motor portion of the trigeminal nerve, which supplies the muscles of mastication as well as mylohyoid, anterior belly of the digastric, tensor veli palatini, and tensor tympani muscles (19). The smaller motor root of the trigeminal exits the pons at the root entry zone of the trigeminal nerve medial to the larger sensory root. It travels to the trigeminal ganglion along the same course as the sensory root but in reverse direction. It bypasses the trigeminal ganglion and exits the skull base through the foramen oval as an individual root. Immediately below the foramen the motor root unites with the sensory root of V3. It descends within V3 between the tensor veli palatine and the lateral pterygoid muscles and then divides into its muscular branches (14, 15).

The evaluation of the cadaver specimens also showed a constant and extensive pericavernous venous plexus around the trigeminal ganglion and the proximal branches of V2 and V3. It is located outside the cavernous sinus but has a direct communication to it (11).

Imaging of the Trigeminal Nerve

The concept of a perineural plexus circumferential to a cranial nerve is not new. Previous studies have

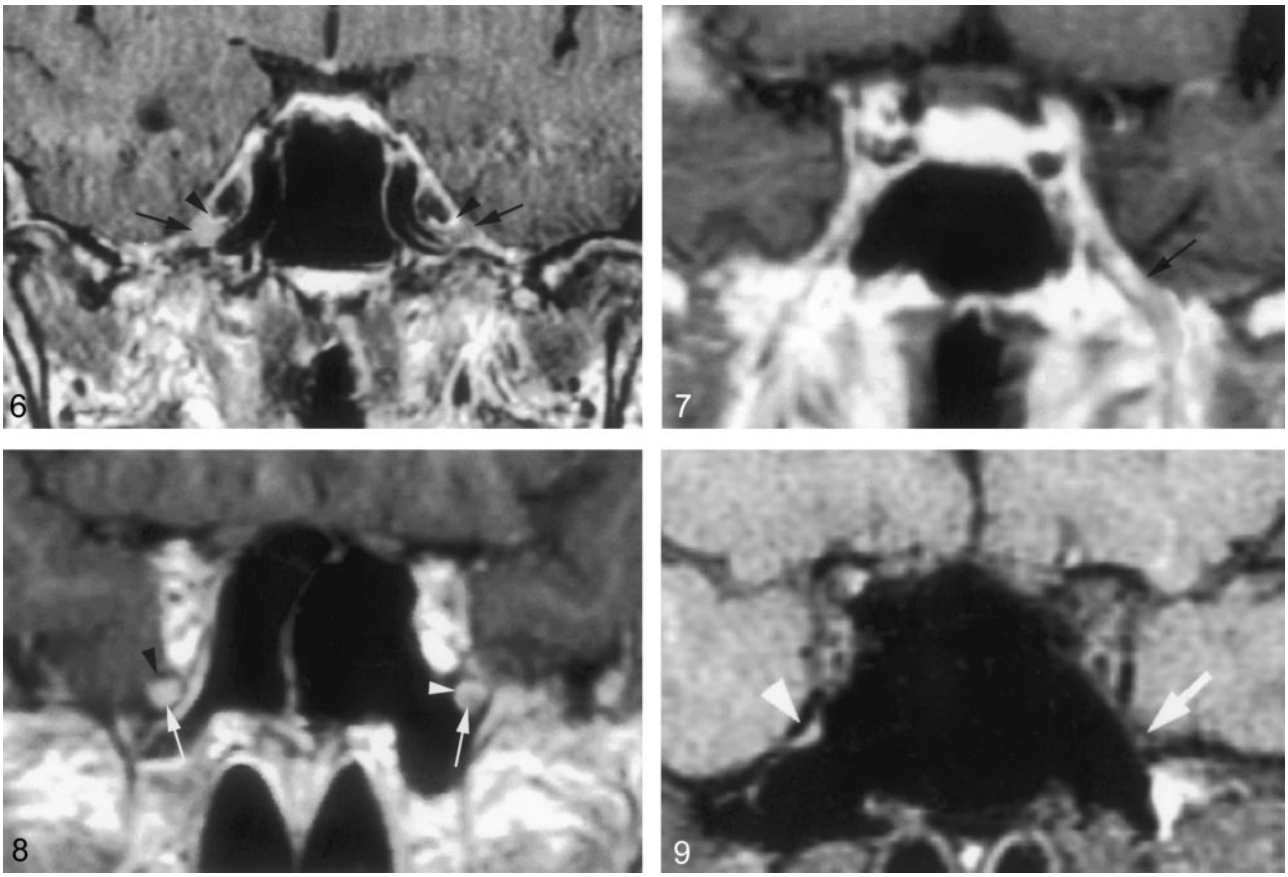

FIG 6. Coronal gadolinium-enhanced T1-weighted image (TR/TE/NEX, 400/15/2) suggests a significantly enhancing right trigeminal ganglion (*right arrow*). The perineural venous plexus (*right arrowhead*) and the trigeminal ganglion cannot be identified as separate structures. This appearance is thought to be due to obscuration of the ganglion by a more extensive perineural venous plexus than that typically seen. The subject did not have any symptoms related to trigeminal nerve or a history of malignancy. Therefore, this is considered a normal variation in imaging appearance. The contralateral side demonstrates the typical appearance of the trigeminal ganglion (*left arrow*) and of adjacent venous plexus (*left arrowhead*).

FIG 7. Coronal gadolinium-enhanced T1-weighted image (TR/TE/NEX, 500/15/2) at the level of the foramen ovale shows a significantly enhancing V3 branch (*arrow*) on the left as a normal anatomic variation. The patient did not have any symptoms of V3 dysfunction. The perineural venous plexus and V3 cannot be seen as individual structures.

FIG 8. Coronal gadolinium-enhanced T1-weighted image (TR/TE/NEX, 500/15/2) at the level of the foramen rotundum demonstrates an enhancing V2 branch on the right when compared with the left (*arrows*). This is considered to represent a normal anatomic variation, because the subject did not have any symptoms related to V2 dysfunction or history of malignancy. The perineural venous plexus and V2 cannot be separated from each other. This appearance might be caused by a more prominent venous plexus. On the left, the perineural venous plexus (*white arrowhead*) is incomplete and absent in the inferior lateral aspect. The *black arrowhead* indicates the bony boundary of the foramen rotundum.

FIG 9. Coronal T1-weighted image (TR/TE/NEX, 753/14/2) through the foramen rotundum demonstrating normal appearing V2 on the left (*arrow*). No nerve can be visualized within the foramen rotundum on the right (*arrowhead*).

reported similar perineural vascular plexuses surrounding other cranial nerves. In the anatomic literature, a "circumneural facial arteriovenous plexus" along the facial nerve in the facial canal has been well described. Gebarski et al (20) compared reference anatomic sections with those of MR images acquired in healthy patients to show that this "circumneural facial arteriovenous plexus" was responsible for the normal MR enhancement along some segments of the facial nerve. Other works on the trigeminal nerve have alluded to the presence of normal MR contrast enhancement in the skull base foramen and attributed it to small dural sinuses and emissary veins that accompany the nerves within their skull base foramina (2). The results of cadaver specimen dissections in this study clarify that the enhancement within the skull base foramina and around the trigeminal ganglion is a vascular plexus engulfing the ganglion and the proximal V1 and V2 branches with drainage into the cavernous sinus (Fig 1).

Downs et al (10) have suggested that enhancement of the trigeminal ganglion is normal and routinely visible on MR images. Conversely, the present study shows that enhancement of the ganglion (Fig 6) and V3 was very uncommon (Fig 7), occurring 4% and 3%, of the time, respectively, and that V2 enhancement (Figs 8 and 9) was seen only 18% of the time. The discrepancy might be due to mistaking the normal and prominent enhancement of perineural vascular plexus surrounding the ganglion for enhancement of the

ganglion itself. This is supported by the observation that complete dissection and removal of the pericavernous venous plexus in the specimens in this study showed no gross or otherwise obvious vascularity in the trigeminal ganglion and proximal V2 and V3 (Fig 1B). Alternatively, this could be related to suboptimal imaging parameters or a combination of both factors.

The present study shows the trigeminal ganglion-nerve and its perineural plexus complex to measure in the range of about 2–3 mm. Optimal visualization and resolution of these structures therefore requires a focused examination, preferably with MR imaging because of its superior tissue contrast and multiplanar capabilities (21, 22). Imaging must consist of sections no thicker than 3–4-mm with a field of view no larger than 16–18 cm. Such parameters should routinely permit visualization of the trigeminal nerve at the skull base and its larger, named, distal branches within the soft tissues as observed in this study. Higher resolution techniques should provide even more fidelity in evaluating these structures.

The imaging parameters mentioned above, in combination with knowledge of frequency of normal enhancement of the trigeminal ganglion and its branches, are crucial for evaluation of patients with suspected trigeminal nerve disease such as perineural tumor spread of skin cancer, which is most commonly seen along the V2 and V3 division of the trigeminal nerve (2). Prior literature establishes abnormal enhancement of a nerve, as well as enlargement of the nerve obliteration of the normal fat plane surrounding the nerve, erosion or enlargement of its related foramen, or abnormal enhancement or mass within the trigeminal cistern or at the root entry zone of the trigeminal nerve as reliable imaging signs of perineural tumor (4, 23). Occasionally and whether actual or apparent, enhancement of the ganglion or proximal V2 and V3 divisions without nerve enlargement or foraminal changes may be seen. This study would suggest that such enhancement could be a normal variant (Figs 6, 7, and 8). This occasional enhancement may be due to avid contrast uptake in an unusually prominent or extensive perineural vascular plexus that obscures the relative lower signal intensity of the nerve it surrounds. A subacute or asymptomatic neuritis (eg, indolent herpes trigeminus) could in theory also produce isolated nerve enhancement. Head tilt and rotation may also artifactually create the appearance of an abnormally enhancing nerve that could be mistaken for perineural spread (2). Careful evaluation of the head positioning and evaluation of the nerve antegrade and retrograde for additional abnormality suggestive of perineural spread will aid in determining whether these findings represent disease or a normal variation or are explained by some other factors or disease processes.

Conclusion

This study characterizes the normal MR appearance of the trigeminal ganglion nerve complex and the perineural vascular plexus of the proximal divisions of V2 and V3 with correlation to cadaver specimens. The trigeminal ganglion is clearly and reliably seen on MR images and very infrequently enhances. Occasional enhancement of V2 is seen, and enhancement of V3 is uncommon. The perineural vascular plexus of V2 and V3 is routinely seen on MR images.

References

1. Soeira G, Abd el-Bary TH, Dujovn M, et al. **Microsurgical anatomy of the trigeminal nerve.** *Neurol Res* 1994;16:273–283
2. Ginsberg LE, DeMonte F. **Imaging of perineural tumor spread from palatal carcinoma.** *AJNR Am J Neuroradiol* 1998;19:1417–1422
3. Laine FJ, Braun IF, Jensen ME, et al. **Perineural tumor extension through the foramen ovale: evaluation with MR imaging.** *Radiology* 1990;174:65–71
4. Caldemeyer KS, Mathews VP, Righi RR, Smith R. **Imaging features and clinical significance of perineural spread or extension of head and neck tumors.** *Radiographics* 1998;18:97–110
5. Majoie CB, Verbeeten B Jr, Dol JA, Peeters FL. **Trigeminal neuropathy: evaluation with MR imaging.** *Radiographics* 1995;15:795–811
6. Kilgore DP, Breger RK, Daniels DL, et al. **Cranial tissues: normal MR appearance after intravenous injection of Gd-DTPA.** *Radiology* 1986;160:757–761
7. Kapila A, Chakeres DW, Blanco E. **The Meckel cave: computed tomographic study. Part I: normal anatomy; part II: pathology.** *Radiology* 1984;152:424–433
8. Rubenstein D, Stears RL, Stears JC. **Trigeminal nerve and ganglion in the Meckel cave: appearance at CT and MR imaging.** *Radiology* 1994;193:155–159
9. Daniels DL, Pech P, Pojunas KW, et al. **Trigeminal nerve: anatomic correlation with MR imaging.** *Radiology* 1986;59:577–583
10. Downs DM, Damiano TR, Rubinstein D. **Gasserian ganglion: appearance on contrast-enhanced MR.** *AJNR Am J Neuroradiology* 1996;17:237–241
11. Haines SJ, Jannetta PJ, Zorub DS. **Microvascular relations of the trigeminal nerve: an anatomical study with clinical correlation.** *J Neurosurg* 1980;42:381–386
12. Agresti A. **Models for matched pairs.** In: Agresti A, ed. *Symmetry Models: Categorical Data Analysis.* New York: John Wiley & Sons; 1990:409–454
13. Agresti A. **Building and extending loglinear? Logit models.** In: Agresti A, ed. *Empty Cells and Sparseness in Contingency Tables. Categorical Data Analysis.* New York, Ny: John Wiley & Sons; 1990;357–408
14. Moore KL, Dalley AF. **Head and neck.** In: Moore KL, Dalley AF, eds. *Clinically Oriented Anatomy.* 4th ed. Philadelphia: Lippincott Williams & Wilkins; 1999;1093–1096
15. Kaufman B, Bellon EM. **The trigeminal nerve cistern.** *Radiology* 1973;108:597–602
16. Kehrli P, Maillot C, Wolff MJ. **The venous system of the lateral sellar compartment (cavernous sinus): an histological and embryological study.** *Neurol Res* 1996;18:387–393
17. Snell RS. **Head and neck.** Snell RS, ed. *Clinical Anatomy for Medical Students.* Boston: Little, Brown; 1995:662–664
18. Wilson-Pauwels L, Akesson E, Stewart P, Spacey S. **Trigeminal nerve.** In: Wilson-Pauwels L, Akesson E, Stewart P, Spacey S, eds. *Cranial Nerves in Health and Disease.* Toronto: B.C. Decker Inc; 2001:50–69
19. Rhoton A. **The cavernous sinus, the cavernous venous plexus, and the carotid collar.** *Neurosurgery* 2002; 51(4 suppl):S375–S410
20. Gebarski SS, Telian SA, Niparko JK. **Enhancement along the normal facial nerve in the facial canal: MR imaging and anatomic correlation.** *Radiology* 1992;183:391–394
21. Davis SB, Mathews VP, Williams DW. **Masticator muscle enhancement in subacute denervation atrophy.** *AJNR Am J Neuroradiol* 1995;16:1292–1294
22. Russo CP, Smoker WRK, Weissman JL. **MR appearance of trigeminal and hypoglossal motor denervation.** *AJNR Am J Neuroradiol* 1997;18:1375–1383
23. Sohn Williams L, Mancuso AA, Mendenhall WM. **Perineural spread of cutaneous squamous and basal cell carcinoma: CT and MR detection and its impact on patient management and prognosis.** *Int J Radiation Oncology Biol Phys* 2001;49:1061–1069